The increase in diffraction efficiency of an azobenzene side-chain polymer using imidazolium and ammonium ionic liquids

Kim, Sung Ho
Department of Chemistry, Kwangwoon University

Kim, Soyeon
Department of Chemistry, Kwangwoon University

Kim, Namwook
Department of Chemistry, Kwangwoon University

Attri, Pankaj
Center of Plasma Nano-interface Engineering, Kyushu University

他

出版情報：Journal of Saudi Chemical Society. 26 (3), pp.101485-, 2022-05. Elsevier
バージョン：

Journal of Saudi Chemical Society (2022) **26**, 101485

King Saud University

Journal of Saudi Chemical Society

www.ksu.edu.sa
www.sciencedirect.com

ORIGINAL ARTICLE

The increase in diffraction efficiency of an azobenzene side-chain polymer using imidazolium and ammonium ionic liquids

Sung Ho Kim [a], Soyeon Kim [a], Namwook Kim [a], Pankaj Attri [b,*], In Tae Kim [a,*]

[a] *Department of Chemistry, Kwangwoon University, Seoul 139-701, South Korea*
[b] *Center of Plasma Nano-interface Engineering, Kyushu University, Fukuoka 819-0395, Japan*

Received 24 March 2022; revised 2 May 2022; accepted 8 May 2022
Available online 13 May 2022

KEYWORDS

Photosensitive;
Azobenzene;
Ionic liquids;
Diffraction efficiency

Abstract The advancement of the information age has intensified the focus on photosensitive materials for information storage devices. To develop new photosensitive two azobenzene side-chain polymers i.e., poly(*E*)-3-(4-((4-nitrophenyl)diazenyl)phenoxy)propyl acrylate (polymer-1) and poly(*E*)-3-(4-((2-methoxy-4-nitrophenyl)diazenyl)phenoxy)propyl acrylate (polymer-2), were developed, and their diffraction efficiency was evaluated. The impact of ionic liquids (ILs) on the diffraction efficiency was evaluated by combining the polymers with imidazolium and ammonium families of ILs such as 1-butyl-3-methylimidazolium bromide [Bmim]Br, 1-ethyl-3-methyl-imidazolium-bromide [Emim]Br (imidazolium ILs), and triethylammonium methanesulfonate [TMEAS] (ammonium IL). The molecular interaction of both azobenzene side-chain polymers with the ILs was evaluated before the diffraction efficiency studies by employing UV–vis, FT-IR, and confocal Raman spectroscopies. The spectroscopic studies revealed the interaction of the polymers with the imidazolium and ammonium ILs. The mean diffraction efficiency of polymers-1 and −2 were ~0.05 and ~0.022%, respectively. After the addition of the ILs, the diffraction efficiency increased. The highest diffraction efficiency was achieved with the polymer-2 + [Emim]Br system of 3.5% and polymer-2 + TEMS combination of 4.03%. Therefore, although the diffraction efficiency of polymer-1 was higher than that of polymer-2, after adding the ILs, the diffraction efficiency of polymer-2 surpassed that of the polymer-1 + ILs system.

1. Introduction

The photosensitive materials are most popular to achieve large-scale data storage and transmission at low cost [1]. Laser modified the optical reflection of the photosensitive materials in both metallic and polymeric form [2,3]. Holographic recording materials like photopolymers and silver halide have high

* Corresponding authors.
E-mail addresses: chem.pankaj@gmail.com (P. Attri), itkim@kw.ac.kr (I.T. Kim).

Peer review under responsibility of King Saud University.

ELSEVIER Production and hosting by Elsevier

https://doi.org/10.1016/j.jscs.2022.101485

sensitivity and high resolution [4]. Azobenzene side-chain polymers displayed their potential applications in various fields in recent years [1–3]. Azobenzene side-chain polymer films hold the unique properties of photoinduced anisotropic effects (where the *trans* configuration (more stable) undergoes a transition to the *cis*-form (less stable) through the excited states) and nonlinearity that makes it favorable holographic recording materials [5–11]. Irradiation with an interfering laser beam results in sinusoidal surface patterns, resulting in the SRG formation [3,7,8]. The azobenzene side-chain polymeric chains' motion induces the unconventional response because of free volume expansion in the bulk lead by isomerization [12,13]. Although azobenzene side-chain polymers still lack high-quality photoinduced anisotropy that is important for the practical use of azobenzene side-chain polymers in optical storage. Therefore, the combination of azobenzene molecules and liquid crystals are used for several applications in optics and information technologies [14–19].

Another class of liquid crystals is Ionic liquids (ILs) which exhibit photoinduced anisotropy. ILs can be considered classical molten salts with distinct chemical compositions and applications [20–22]. Pan et al. reported the azo-containing IL-crystalline polymer for long-term optical storage [23]. Zhao et al. developed the azo-containing IL-crystalline polymer film that displayed enormous nonlinear refraction and negligible nonlinear absorption [24].

In our ongoing studies, we focused on the interaction of ILs with different synthesized polymers [21,25–27]. The low band-gap polymer (Poly(2-heptadecyl-4-vinylthieno[3,4-d]thiazole) interacted with tributylmethylammonium methyl sulfate, 1-methylimidazolium chloride ([Mim]Cl), and 1-butyl-3-methylimidazolium chloride ([Bmim]Cl), which reveals that [Mim]Cl strongly interact with polymer than other ILs [21]. Additionally, we showed the interaction of thiophene-based conducting polymer (2-heptadecyl-5-hexyl-6-(5-methylthio phen-2-yl)-4-(5-((E)-prop-1-enyl)thiophen-2-yl)-5H-pyrrolo[3, 4-d]thiazole) with 1-butyl-3-methylimidazolium bromide [Bmim]Br, 1-ethyl-3-methyl-imidazolium-bromide [Emim]Br, triethylammonium methanesulfonate [TMEAS], and tributyl-methylammoniummethyl sulfate ILs [26]. Recently, we showed the interaction of [Bmim]Br, [Emim]Br and TMEAS ILs with lowband gap polymer, poly(2-heptadecyl-4-vinyl thieno[3,4-d] [1,3] selenazole) [27]. Moreover, in the earlier study we showed the diffraction efficiency of the epoxy-based polymer with and without addition of ILs ([Mim]Cl, diethylammonium dihydrogen phosphate, tributylmethylammonium methylsulphate and triethylammonium 4-aminotoluene-3-sulfonic acid) [28]. Although we observed only diethylammonium dihydrogen phosphate IL combination with the epoxy-based polymer could increase the diffraction efficiency to 0.07% [28]. This shows huge scope for improving polymer diffraction efficiency alone or in combination with ILs.

Therefore, we herein study the interaction between a newly synthesized azobenzene side-chain polymers (azobenzene side-chain polymer 1 and azobenzene side-chain polymer 2) (see Fig. 1), with ILs (imidazolium (1-butyl-3-methylimidazolium bromide [Bmim]Br, 1-ethyl-3-methyl-imidazolium-bromide [Emim]Br) and ammonium triethylammonium methanesulfonate [TMEAS] families) using UV–vis, FT-IR, and confocal Raman spectroscopies. Furthermore, we investigate the SRG and diffraction efficiency of azobenzene side-chain polymers and azobenzene side-chain polymer-IL mixtures.

2. Materials and methods

2.1. Materials

Acryloyl chloride, phenol, aniline, 4-nitrobenzenediazonium tetrafluoroborate, [Bmim]Br, [Emim]Br and 3-chloro-1-propanol were purchased from Sigma-Aldrich, Co. All the other materials, reagents, and solvents were commercially available products and were used as received without further purification. The synthesis of azobenzene side-chain polymer-1 and polymer-2 is described below and illustrated in Fig. 1.

2.2. Synthesis of the azobenzene side-chain polymers

(*E*)-3-(4-((4-Nitrophenyl)diazenyl)phenoxy)propan-1-ol was prepared from (*E*)-4-((4-nitrophenyl)diazenyl)phenol and 3-bromopropanol according to the method described by Tochitsky and coworkers [29].

Synthesis of Compound 1 (Compound 2): (*E*)-3-(4-((4-Nitro phenyl)diazenyl)phenoxy)propan-1-ol (2.7 g, 0.0081 mol) in anhydrous tetrahydrofuran (THF) was combined with triethylamine (5.58 ml, 0.04 mol) under nitrogen atmosphere at 0℃.

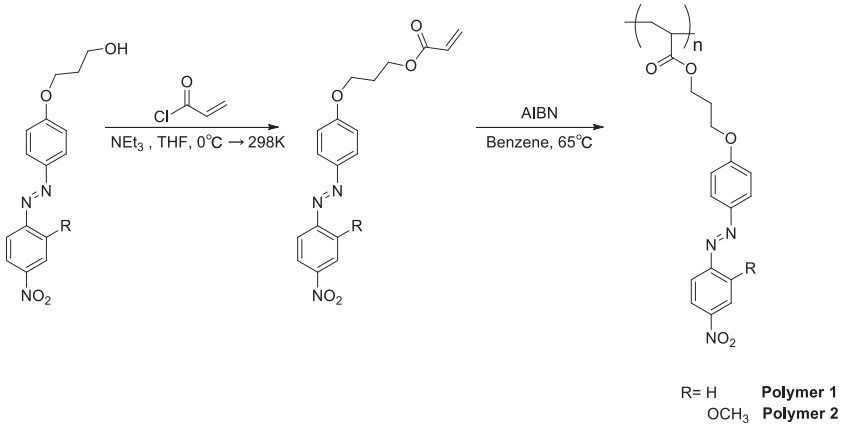

Fig. 1 Synthesis of azobenzene side-chain polymers.

Acryloyl chloride (3.9 ml, 0.04 mol) was added dropwise to the solution and stirred overnight at room temperature (RT). The resultant mixture was evaporated to eliminate THF. The product was washed with chloroform and HCl several times. The combined organic extracts were dried over $MgSO_4$. The residue was purified by column chromatography using silica gel as the absorbent, and a solvent mixture comprising ethylacetate/*n*-hexane (*v*/*v* = 30/70) was used as the eluent in this chromatographic technique. The yield of compound 1 was 1.23 g (yield: 43% (64% for compound 2).

Compound 1 ^{1}H NMR (400 MHz, $CDCl_3$) δ 8.36 (d, 2H), 7.98 (d, 2H), 7.97 (d, 2H), 7.03 (d, 2H), 6.43 (d, 1H), 6.14 (t, 1H), 5.85 (d, 1H), 4.40 (t, 2H), 4.18 (t, 2H), 2.23(m, 2H); ^{13}C NMR (100 MHz, $CDCl_3$) δ 166, 162, 155, 148, 146, 131, 128, 125, 124, 123, 114, 64, 61, 28).

Compound 2 ^{1}H NMR (400 MHz, $CDCl_3$) δ 7.98 (d, 2H), 7.93 (d, 2H), 7.70 (d, 1H), 7.04 (d, 2H), 6.13 (d, 1H), 5.59 (s, 1H), 4.40 (d, 2H), 4.20 (d, 2H), 4.11 (s, 3H), 2.26 (m, 2H); ^{13}C NMR (100 MHz, $CDCl_3$) δ 167, 162, 156, 149, 147, 146, 136, 125, 117, 116, 114, 107, 64, 64, 61, 60, 56, 40, 31.

Synthesis of azobenzene side-chain polymer1 (polymer-1): Compound 1 (2 g, 0.0052 mol) in anhydrous benzene was combined with AIBN (1.7 g; 0.01 mol) under a nitrogen atmosphere. The mixture was stirred for 3 d at 65℃; the resultant mixture was evaporated to eliminate benzene. The product was washed with methanol several times. Finally, ~0.2 g of azobenzene side-chain polymer 1 was obtained 40% yield. ^{1}H NMR (400 MHz, $CDCl_3$) (see Fig. S1) δ 8.32 (s, 2H), 7.92 (s, 4H), 6.98 (s, 2H), 4.26 (s, 2H), 4.09 (s, 2H), 2.17 (m, 3H), 1.31 (Ss, 1H); ^{13}C NMR (100 MHz, $CDCl_3$) δ 125, 124, 123, 114, 72, 72, 70, 70, 70, 70, 61, 61, 29.

Synthesis of azobenzene side-chain polymer2 (polymer-2): Compound 2 (2 g, 0.0052 mol) in anhydrous benzene was combined with AIBN (1.7 g 0.01 mol) under a nitrogen atmosphere. The mixture was stirred for 3 d at 65℃; the resultant mixture was evaporated to eliminate benzene. The product was washed with methanol several times. Finally, ~1.0 g of azobenzene side-chain polymer 2 was obtained 50% yield. ^{1}H NMR (400 MHz, $CDCl_3$) (see Fig. S2) δ 7.97 (m, 4H), 7.70 (d, 2H), 7.04 (d, 2H), 4.38 (d, 2H), 4.18 (d, 2H), 4.11 (s, 3H), 2.16 (s, 2H); ^{13}C NMR (100 MHz, $CDCl_3$) δ 162, 156, 149, 147, 146, 125, 117, 116, 114, 107, 64, 64, 61, 61, 56, 40, 31).

2.3. Characterization

JEOL MSL 300 spectrometer was used to detect the ^{1}H NMR and ^{13}C NMR spectra. Polystyrene standards in tetrahydrofuran solutions are used as the standards for gel permeation chromatography. Thermogravimetric analysis (Shimadzu TGA-50 series), (UV–Vis (S-3100), FTIR (Bomem MB Series MB100), and confocal Raman (WITec, Alpha 300 R) measurements are described in our earlier work [21,26]. The major products were isolated by flash column chromatography on silica gel (230–400 mesh ATSM, purchased from Merck & Co., Inc. (Whitehouse Station, New Jersey, USA)) using a mixed solvent eluent (chloroform/acetone (*v*/*v* = 95/5)). Gel permeation chromatography (GPC) data were obtained with a Waters 1515 (Waters) instrument. The laser experiment was conducted with a diode-pumped solid-state (DPSS) laser (Genesis CX-Series SLM; Coherent Lasers, Santa Clara, CA, USA).

2.4. Experimental setup

The azobenzene side-chain polymer's homogeneous solutions in anhydrous tetrahydrofuran with a typical concentration of 12 wt% were filtered through 0.45 μm membranes and bar-coated onto normal glass slides. The average film thickness was varied from experiment to experiment. The coated films were dried at 100 °C in an oven for 24 h before use. The experimental setup used to realize and optimize SRG formation was described in previous work [28]. The interference of two coherent beams (λ = 488 nm) was used to inscribe the SRG on the azobenzene side-chain polymer films. The angle between the two beams (2θ) was 45°, resulting in a grating period of about 2 μm. The intensity of each writing beam measured at the sample position was about 171 mW. To monitor SRG formation, the sample surface was irradiated with low power (0.11 mW) laser beam (λ = 660 nm), and the first-order diffraction signal was measured. Herein, the probing beam used for SRG fabrication was s- or p-polarized. SRG engraving was carried out under ambient conditions at room temperature. The diffraction efficiency was measured during SRG formation as a function of the photo-irradiation time.

3. Results and discussion

3.1. TGA and UV–Vis study of polymer-1 and polymer-2 with and without ILs

Two azobenzene side-chain polymers that are used as holographic recording materials were synthesized herein. Two different types of azobenzene side-chain polymers (polymer-1 and polymer-2) were introduced into the precursor polymer via an azo coupling reaction (as shown in Fig. 1). The synthesized azobenzene side-chain polymers are short linear polymers with a molecular weight of around 10,000. The respective yields of polymer-1 and polymer-2 were 40 and 50%; the degree of functionalization of both azobenzene side-chain polymers was estimated using ^{1}H NMR analysis. The thermogravimetric analysis (TGA) data indicated the polymer-1 mass loss of ~49.9% up to a temperature of 499 °C and polymer-2 mass loss of ~59.7% up to a temperature of 400 °C. The polymer efficiency (polymer-1 and polymer-2) was determined by UV–vis spectroscopy. The λ_{max} values for polymer-1 and polymer-2 in THF solution were 348 and 351 nm, as shown in Fig. 2. The π-π* absorption band appeared at a longer wavelength in the visible region, as indicated by the λ_{max} value; this may be due to the donor–acceptor-type azo chromophores. Hence, λ_{max} for polymer-2 was slightly red-shifted compared with polymer-1, which might be due to the electron donation group (methoxy) in the *o*-position of the azo-benzene units. Moreover, after the interaction of the ILs with polymer-1 and polymer-2, the UV–vis spectra were not strongly red- or blue-shifted. However, after the interaction of ILs with the azobenzene side-chain polymers, the peak-width increased/decreased. For polymer 1 + [Bmim]Br, and + [Emim]Br, no peak shift was observed, and there was no change in the peak shape. For polymer-1 + TEMS IL, the peak-width decreased but λ_{max} remained the same. This reveals that neither family of ILs (imidazolium and ammonium) had a strong interaction with polymer-1 (λ_{max} was the same before and after mixing with the ILs); however, the decreased peak-width observed

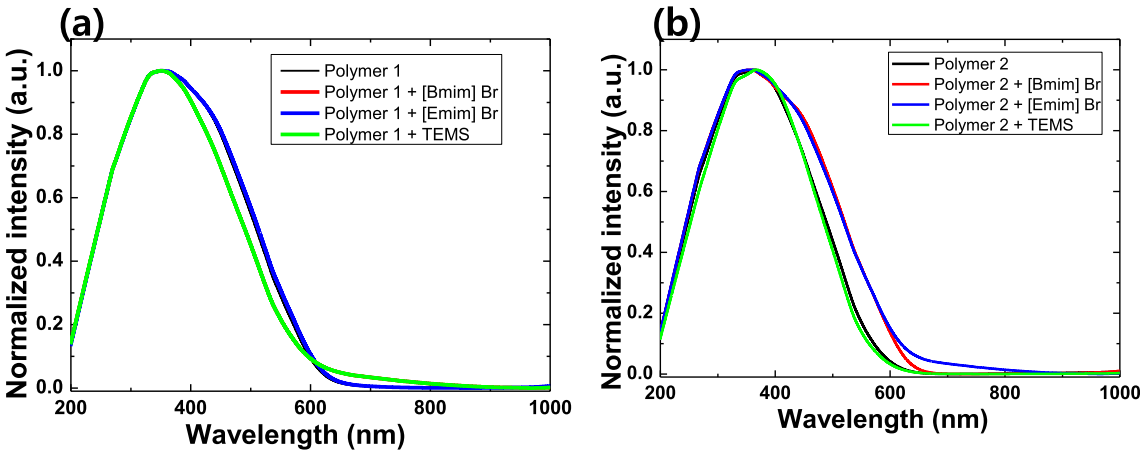

Fig. 2 UV–Vis spectra of the (a) polymer-1 and polymer-1 + ILs and (b) polymer-2 and polymer-2 + ILs.

with the ammonium IL may be due to interaction with polymer-1.

No red/blue shift of the peak of polymer-2 was observed in the UV–vis spectra of the azobenzene side-chain polymer-2 + ILs (after interaction with the ILs), except in the case of TEMS. A slight red-shift was observed for polymer-2 + TEMS; the λ_{max} for polymer-2 was 351 nm, whereas λ_{max} for polymer-2 + TEMS was 366 nm. Hence, for polymer-2 + TEMS, the peak was red-shifted by 15 nm compared to polymer-2. On the contrary, the TEMS + polymer-2 did not decrease the peak width than polymer-2 itself. This behavior is opposite to the above case, where TEMS caused no red-shift but decreased the peak-width upon interaction with azobenzene side-chain polymer 1. However, after the interaction of polymer-2 with [Bmim] Br and [Emim] Br, the polymer peak width increased compared to polymer-2 itself, while λ_{max} was the same for the mixtures and polymer-2. This reveals that both families of ILs, i.e., [Bmim] Br, [Emim] Br (imidazolium family) and the TEMS (ammonium) family, undergo interactions with polymer-2, as indicated by the shift in λ_{max} as well as the increased peak-width. FT-IR and confocal Raman spectroscopies were used for a more in-depth analysis of the molecular interactions.

3.2. Interaction studies between azobenzene side-chain polymers and ILs

The molecular interaction between the azobenzene side-chain polymers and ILs are studied using FT-IR and confocal Raman spectroscopies. The FT-IR spectra of azobenzene side-chain polymer-1 with and without ILs, shown in Fig. 3a.

The peaks of polymer-1 at 2921, 1734, 1496, 1336, 1241, 1123, and 826 cm^{-1} are assigned to CH_3, CH_2, & CH (stretching vibrations), ester (C = O stretch), NO_2 (asymmetric), CH_2 & CH_3 deformation (bending vibrations), CO-O (stretching absorptions), O-C (stretching vibrations), and aromatic p-substituent, respectively. After the interaction of polymer-1 with [Bmim]Br and [Emim]Br, the peak positions did not change; only an increase in the intensity at 1734 cm^{-1} and a decrease in intensity at 2921 cm^{-1} for polymer-1 + [Emim] Br was noticed. However, after the interaction of polymer-1 with TEMS, peak shifts were observed at 2956 and 1488 cm^{-1}, and the peak at 1123 cm^{-1} disappeared. Additionally, the 1734 cm^{-1} peak intensity increased, whereas the peak at 2921 cm^{-1} became less intense for polymer-1 + TEMS. Thus, the interaction of polymer-1 with TEMS results in a peak shift and change in the peaks' intensity. These results correlate with the UV–Vis spectra, where TEMS induces a red-shift of the peaks of polymer-1, whereas [Bmim]Br and [Emim]Br do not shift λ_{max} for polymer-1.

On the other hand, for polymer-2, peaks were observed at (2931, 2856), 1734, 1500, 1342, 1249, (1131, 1028), and 842 cm^{-1} assigned to the CH_3, CH_2 & CH (stretching vibrations), ester (C = O stretch), NO_2 (asymmetric), CH_2 & CH_3 deformation (bending vibrations), CO-O (stretching absorptions), O-C (stretching vibrations), and aromatic p-substituent, respectively, as shown in Fig. 3b. For polymer-2 + [Bmim]Br, the peak shift at 2946 cm^{-1}, whereas polymer-2 + [Emim]Br, the peaks shift at 1733 and 2955 cm^{-1}, and peak intensity at 1733 cm^{-1} increased for polymer-2 + [Emi m]Br. Moreover, the interaction of polymer-2 with TEMS induced peak shifts at 1741 and 2955 cm^{-1}. Thus, peak shifts were observed for all the polymer-2 + IL mixtures relative to those of polymer-2 itself. Hence, polymer-2 undergoes strong interactions with all ILs, whereas polymer-1 undergoes strong interactions with TEMS. Confocal Raman spectroscopy is used to understand the interactions further.

Raman scattering and attenuation of the excitation laser power were indicated by the Raman signal's strong attenuation with increasing penetration of the membrane polymer. Fig. 4a shows significant peaks at 1140, 1248, 1341, (1410, 1454), and 1583 cm^{-1} that correspond to υ(C-O-C) asym, υ (CC) aliphatic chain vibration, υ(C-NO_2), δ(CH_2)δ(CH_3) asym, and υ(N = N), respectively. After the interaction of polymer-1 with the ILs ([Bmim]Br, [Emim]Br, and TEMS), no peak shift was observed. In contrast, for polymer-2, Raman peak shifts were observed at 1143, 1247, 1341, (1410, 1454), and 1586 cm^{-1}, which correspond to υ(C-O-C) asym, υ(CC) aliphatic chain vibration, υ(C-NO_2), δ(CH_2)δ(CH_3) asym, and υ(N = N), respectively, as shown in Fig. 4b. Even after the interaction of the ILs ([Bmim]Br, [Emim]Br, and TEMS) with azobenzene side-chain polymer 2, no significant peak shift was observed. Hence, no Raman peak shift was observed for polymer-1 and polymer-2 after the addition of the ILs.

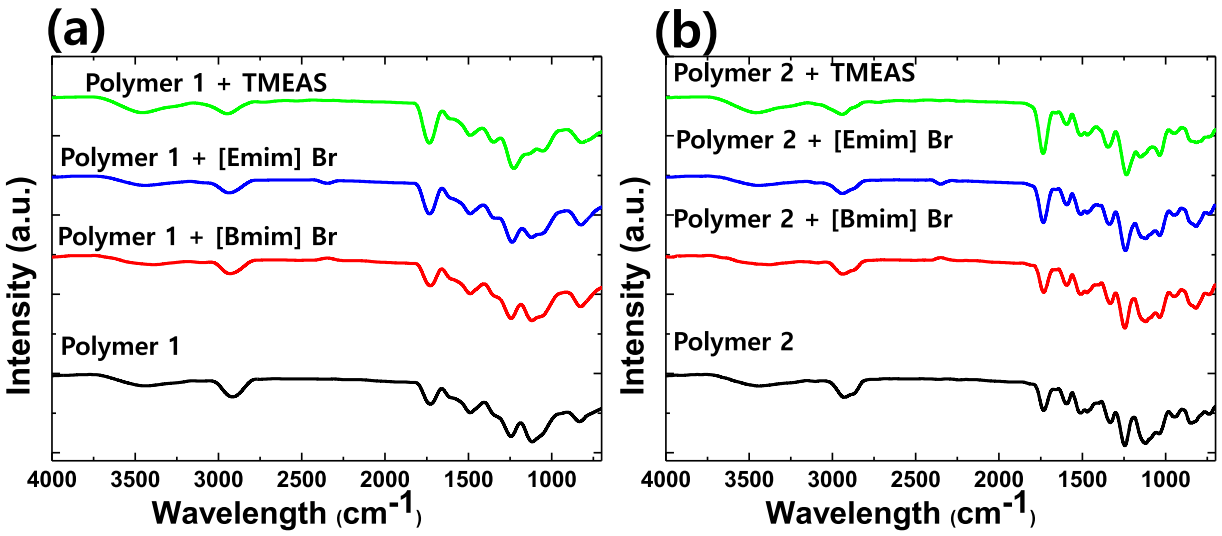

Fig. 3 FTIR spectra of the (a) polymer-1 and polymer-1 + ILs and (b) polymer-2 and polymer-2 + ILs.

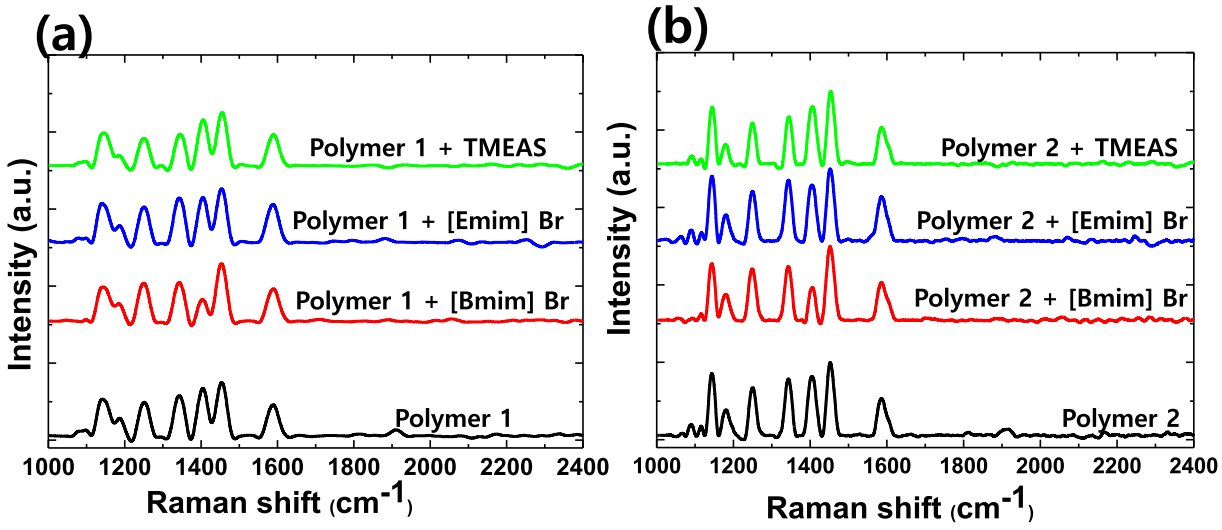

Fig. 4 Confocal Raman spectroscopy data of (a) polymer-1 and polymer-1 + ILs and (b) polymer-2 and polymer-2 + ILs.

The interaction of ILs with polymers (polymer-1 and polymer-2) revealed that Π-Π interaction was more vital for imidazolium-based ILs with both polymer-1 and polymer-2. However, UV–vis and FTIR studies showed strong interaction of polymer-1 with TEMS than [Emim]Br and [Bmim]Br, which may be due to the role of H-bonding. Possible strong H-bonding between the TEMS and polymers (polymer-1 and polymer-2).

3.3. Analysis of diffraction efficiency of polymer-1 and polymer-2 under different conditions

The diffraction efficiency was measured during surface-relief-grating (SRG) formation with respect to the photo-irradiation time. The change in the diffraction efficiency with a variation of the writing beam power, recording time, readout beam wavelength, writing beam polarization, film thickness, readout beam power, and the incident angle was evaluated. Table 1 showed the results when a 488 nm DPSS laser was used as the writing beam with an intensity of 171 mW and 410 mW, using a film thickness of 0.5–1 μm. A 488 nm DPSS laser was also used as the readout beam; both the writing and readout beams were s-polarized. The diffraction efficiency increased as the irradiation time increased up to 30 s, then decreased or both azobenzene side-chain polymers when the irradiation beam's intensity was 171 mW. The diffraction efficiency could not be determined when the irradiation beam's intensity was 410 mW under similar conditions for polymers-1 and −2. This might be due to the destruction of the azobenzene side-chain polymer film upon irradiation at an intensity of 410 mW; hence, no diffraction was observable. The impact of varying the writing beam's wavelength and readout beam on the diffraction efficiency was also evaluated, as shown in Table 1 and Table 2. The diffraction efficiency increased when the readout beam's wavelength from the DPSS laser was changed from 488 nm to 660 nm. The data in Table 2 show that

Table 1 Diffraction efficiency of polymer-1 and polymer-2, having 0.5 ~ 1 μm film thickness, 488 nm DPSS laser with s-polarized beam used for both writing and readout with an incident angle of 45°.

Polymer	Intensity of irradiation writing beam (W)	Irradiation time (s)	Intensity of irradiation readout beam (W)	Diffraction efficiency (%)
Polymer-1	0.171	10	1.00E-02	0.0014 ± 0.0001
		14		0.0016 ± 0.0002
		18		0.0026 ± 0.0007
		22		0.0022 ± 0.0001
		26		0.0027 ± 0.0002
		30		0.0029 ± 0.0001
		40		0.0027 ± 0.0001
Polymer-2	0.171	10	1.00E-02	0.0017 ± 0.0001
		14		0.0018 ± 0.0001
		18		0.0020 ± 0.0002
		22		0.0019 ± 0.0003
		26		0.0015 ± 0.0002
		30		0.0015 ± 0.0001
		40		0.0021 ± 0.0004
Polymer-1	0.410	5	not recorded	
		10		
		15		
		20		
		30		
Polymer-2	0.410	5		
		10		
		15		
		20		
		30		

Table 2 Influence of the polarization of writing beam, and polymer structure on diffraction efficiency, having 5 ~ 10 μm film thickness, and 488 and 660 nm DPSS laser for writing beam and readout beam, respectively, with an incident angle of 45°.

Polymer	Polarization of Writing beam	Intensity of irradiation writing beam (W)	Irradiation time (s)	Polarization of readout beam	Intensity of irradiation readout beam (W)	Diffraction efficiency (%)
Polymer-1	**s-polarized beam**	0.171	5	**p-polarized beam**	1.85E-06	0.047 ± 0.001
			10			0.060 ± 0.001
			15			0.056 ± 0.002
			20			0.037 ± 0.010
			30			0.037 ± 0.012
Polymer-2	**s-polarized beam**	0.171	5	**p-polarized beam**	1.85E-06	not recorded
			10			
			15			
			20			
			30			
Polymer-1	**p-polarized beam**	0.171	5	**p-polarized beam**	1.85E-06	0.057 ± 0.003
			10			0.077 ± 0.001
			15			0.060 ± 0.001
			20			0.076 ± 0.002
			30			0.036 ± 0.001
Polymer-2	**p-polarized beam**	0.171	5	**p-polarized beam**	1.85E-06	0.039 ± 0.001
			10			0.055 ± 0.001
			15			0.045 ± 0.001
			20			0.043 ± 0.001
			30			0.035 ± 0.001

changing the writing beam's polarization from s-polarized to p-polarized increased the diffraction intensity.

Moreover, the diffraction efficiency of polymer-1 was higher than that polymer-2 when both the writing beam and readout beam were p-polarized, and the writing wavelength beam and readout beam was 488 and 660 nm, respectively. This might be due to the steric hindrance created by the methoxy group of polymer-2. To understand the polymer film thickness's impact on the diffraction efficiency, azobenzene side-chain polymer films with two different thicknesses (5–10 μm and 0.5–1 μm) were used, as illustrated in Table 3.

The diffraction efficiency of polymer-1 was higher for the thick polymer film than for the thin polymer film because SRG formation is easier for the thick film. However, we could not determine the diffraction efficiency in the case of polymer-2 for the film thickness of 5–10 μm. Additionally, the incident

Table 3 Effect of film thickness on diffraction efficiency using 488 and 660 nm DPSS laser for writing beam and readout beam, respectively, with an incident angle of 45°. The intensity of the irradiation writing beam and readout beam were 0.171 and 1.00 E-02W, respectively.

Polymer	Film thickness	Polarization of Writing beam	Irradiation time (s)	Polarization of readout beam	Diffraction efficiency (%)
Polymer-1	5 ~ 10 μm	**s-polarized beam**	5	**p-polarized beam**	0.047 ± 0.003
			10		0.060 ± 0.001
			15		0.056 ± 0.001
			20		0.037 ± 0.002
			30		0.037 ± 0.003
Polymer-1	0.5 ~ 1 μm	**s-polarized beam**	5	**p-polarized beam**	0.001
			10		0.002 ± 0.001
			15		0.003 ± 0.001
			20		0.002 ± 0.001
			30		0.003 ± 0.001
Polymer-2	5 ~ 10 μm	**s-polarized beam**	5	**p-polarized beam**	not recorded
			10		
			15		
			20		
			30		
Polymer-2	0.5 ~ 1 μm	**s-polarized beam**	5	**p-polarized beam**	0.002 ± 0.001
			10		0.002 ± 0.001
			15		0.002 ± 0.002
			20		0.002 ± 0.001
			30		0.002 ± 0.002

Table 4 Influence of incident angle on diffraction efficiency with 0.5 ~ 1 μm film thickness using 488 and 660 nm DPSS laser for writing beam and readout beam, respectively. Intensity of the irradiation writing beam and readout beam were 0.171 and 1.00 E-01 W, respectively.

Polymer	Polarization of Writing beam	Incident angle (°)	Irradiation time (s)	Polarization of readout beam	Diffraction efficiency (%)
Polymer-1	**p-polarized beam**	20	10	**p-polarized beam**	0.013 ± 0.002
			20		0.011 ± 0.001
			30		0.007 ± 0.002
Polymer-1	**p-polarized beam**	45	10	**p-polarized beam**	0.030 ± 0.001
			20		0.025 ± 0.001
			30		0.025 ± 0.001
Polymer-1	**p-polarized beam**	60	10	**p-polarized beam**	0.018 ± 0.001
			20		0.015 ± 0.002
			30		0.025 ± 0.002
Polymer-2	**p-polarized beam**	20	10	**p-polarized beam**	0.002 ± 0.001
			20		0.003 ± 0.001
			30		–
Polymer-2	**p-polarized beam**	45	10	**p-polarized beam**	0.003 ± 0.001
			20		0.003 ± 0.001
			30		0.002 ± 0.001
Polymer-2	**p-polarized beam**	60	10	**p-polarized beam**	0.004 ± 0.001
			20		0.006 ± 0.001
			30		0.005 ± 0.001

angle's impact on the diffraction efficiency was studied by varying the incident angle as 20, 45, and 60° for both polymers, as shown in Table 4. The maximum diffraction was observed at 45° for both polymers. Hence, for the subsequent studies, we used the incident angle of 45° and film thickness of 0.5–1 μm for polymer-1 or -2 + ILs.

3.4. Analysis of diffraction efficiency under different conditions for polymer-1 + ILs and polymer-2 + ILs

As demonstrated above, the diffraction efficiency can be improved by changing the film thickness and readout beam wavelength and changing the s-polarized writing beam to a p-polarized writing beam. As indicated in Tables 1–4, both polymers' diffraction efficiency was quite low; however, the diffraction efficiency of polymer-2 was lower than that of polymer-1 Therefore, the present work aimed to increase diffraction efficiency via the addition of ILs. Hence, three ILs from the imidazolium family and ammonium family were used herein. Using a writing beam with a wavelength of 488 nm and intensity of 171 mW, the maximum diffraction efficiency was 0.060 ± 0.001% after 5 s of irradiation with a p-polarized readout beam with a wavelength of 660 nm for polymer-1. Under the same conditions, the maximum diffraction efficiency of the polymer-1 + [Bmim]Br, + [Emim]Br and +TEMS systems was 0.090 ± 0.002, 0.14 ± 0.02, and 0.05 ± 0.01% for 5, 5, and 10 s irradiation with the p-polarized readout beam with a wavelength of 660 nm, respec-

Table 5 Influence of the polarization of writing beam and polymer structure on diffraction efficiency with 0.5 ~ 1 μm film thickness using 488 and 660 nm DPSS laser for writing beam and readout beam, respectively, with an incident angle of 45°.

Polymer	Polarization of Writing beam	Intensity of irradiation writing beam (mW)	Irradiation time (s)	Polarization of readout beam	Intensity of irradiation readout beam (W)	Diffraction efficiency (%)
Polymer-1	p-polarized beam	171	5	p-polarized beam	1.18E-02	0.06 ± 0.02
			10			0.04 ± 0.001
			15			0.04 ± 0.001
			20			0.03 ± 0.001
			30			0.06 ± 0.001
Polymer-1 + [Emim]Br	p-polarized beam	171	5	p-polarized beam	1.18.E-02	0.09 ± 0.002
			10			0.07 ± 0.001
			15			0.07 ± 0.001
			20			0.07 ± 0.001
			30			0.04 ± 0.002
Polymer-1 + [Bmim]Br	p-polarized beam	171	5	p-polarized beam	1.18.E-02	0.14 ± 0.02
			10			0.05 ± 0.01
			15			0.05 ± 0.01
			20			0.06 ± 0.01
			30			0.01 ± 0.01
Polymer-1 + TEMS	p-polarized beam	171	5	p-polarized beam	1.18.E-02	0.04 ± 0.01
			10			0.04 ± 0.01
			15			0.05 ± 0.02
			20			0.03 ± 0.01
			30			0.02 ± 0.01
Polymer-2	p-polarized beam	171	5	p-polarized beam	1.18.E-02	0.03 ± 0.01
			10			0.02 ± 0.01
			15			0.02 ± 0.01
			20			0.02 ± 0.01
			30			0.02 ± 0.01
Polymer-2 + [Emim]Br	p-polarized beam	171	5	p-polarized beam	1.18.E-02	–
			10			3.31 ± 0.02
			15			3.64 ± 0.03
			20			3.56 ± 0.01
			30			–
Polymer-2 + [Bmim]Br	p-polarized beam	171	5	p-polarized beam	1.18.E-02	–
			10			3.22 ± 0.02
			15			3.22 ± 0.02
			20			2.54 ± 0.01
			30			–
Polymer-2 + TEMS	p-polarized beam	171	5	p-polarized beam	1.18.E-02	–
			10			3.98 ± 0.03
			15			4.32 ± 0.02
			20			3.81 ± 0.02
			30			–

tively (Table 5). Additionally, as the laser irradiation time increased, the diffraction efficiency decreased. This may be attributed to the more significant heating effect with prolonged irradiation, which affects the interaction between the azo-polymer and ILs.

The diffraction efficiency of polymer-2 was studied under the aforementioned conditions (writing beam: 488 nm wavelength; intensity: 171 mW; wavelength readout beam: 660 nm). The maximum efficiency was 0.03 ± 0.01% for 5 s of irradiation, which was less than that of polymer-1 under the same conditions. These results are quite similar to those of the above study, where the diffraction efficiency of polymer-1 is higher than that of polymer-2. Similar to the above case, the ILs were mixed with polymer-2, and the diffraction efficiency was recorded. The maximum diffraction efficiency was 3.64 ± 0.03, 3.22 ± 0.02, and 4.32 ± 0.02% for the polymer-2 + [Bmim]Br, + [Emim]Br and +TEMS ILs. These results are quite interesting because, as demonstrated by the UV spectra, the behavior of the ILs with polymer-1 and polymer-2 was quite different, although the polymers differ by a methoxy group only. The UV spectra of the polymer-2 + TEMS system were red-shifted and peak shifts were observed in the FTIR spectrum as compared to that of the other IL combinations with polymer-2 or polymer-2 alone. Further, polymer-2 with TEMS exhibited the maximum diffraction efficiency.

4. Conclusion

The extensive experimental data illustrate that two new photosensitive materials were successfully synthesized. Azobenzene side-chain polymers (polymer-1 and polymer-2) exhibit π-π* emission at the same wavelength. The diffraction efficiency studies reveal that the emission depends upon many factors, such as the writing beam power, recording time, readout beam wavelength, polarization of the writing beam, film thickness, readout beam power, and incident angle. Additionally, under the optimized conditions, the diffraction efficiency of polymer-1 is higher than polymer-2, attributed to the steric hindrance created by the methoxy group. Although the addition of the ILs increases the diffraction efficiency for both polymers, the maximum efficiency was obtained for the polymer 2 + ILs. The diffraction efficiency of the polymer-2 + imi dazolium ILs is plausibly due to the strong Π-Π interaction of the azobenzene side-chain polymer with [Bmim]Br and [Emim] Br ILs. In contrast, H-bond plays an essential role in the interaction between polymer-2 and ammonium IL. Although, it is worthy to note that cation plays a vital role in imidazolium ILs interaction with polymer than anion.

Declaration of Competing Interest

The authors declare that they have no known competing financial interests or personal relationships that could have appeared to influence the work reported in this paper.

Acknowledgements

This work was supported by the Korea Institute of Energy Technology Evaluation and Planning (KETEP) and the Ministry of Trade, Industry &Energy (MOTIE) of the Republic of Korea (20173030014460) and Research Grant of Kwangwoon University in (2021). This work is partly supported by JSPS-KAKENHI grant number 22H01212 (PA)

Appendix A. Supplementary data

Supplementary data to this article can be found online at https://doi.org/10.1016/j.jscs.2022.101485.

References

[1] S. Xie, A. Natansohn, P. Rochon, Recent developments in aromatic azo polymers research, Chem. Mater. 5 (1993) 403–411, https://doi.org/10.1021/cm00028a003.
[2] J.A. Delaire, K. Nakatani, Linear and nonlinear optical properties of photochromic molecules and materials, Chem. Rev. 100 (2000) 1817–1845, https://doi.org/10.1021/cr980078m.
[3] A. Natansohn, P. Rochon, Photoinduced motions in azo-containing polymers, Chem. Rev. 102 (2002) 4139–4175, https://doi.org/10.1021/cr970155y.
[4] T. Ikeda, J. Mamiya, Y. Yu, Photomechanics of liquid-crystalline elastomers and other polymers, Angew. Chemie Int. Ed. 46 (2007) 506–528, https://doi.org/10.1002/anie.200602372.
[5] T. Ikeda, S. Horiuchi, D.B. Karanjit, S. Kurihara, S. Tazuke, Photochemically induced isothermal phase transition in polymer liquid crystals with mesogenic phenyl benzoate side chains. 2. Photochemically induced isothermal phase transition behaviors, Macromolecules 23 (1990) 42–48, https://doi.org/10.1021/ma00203a009.
[6] T. Todorov, L. Nikolova, N. Tomova, Polarization holography 1: A new high-efficiency organic material with reversible photoinduced birefringence, Appl. Opt. 23 (1984) 4309, https://doi.org/10.1364/AO.23.004309.
[7] D.Y. Kim, S.K. Tripathy, L. Li, J. Kumar, Laser-induced holographic surface relief gratings on nonlinear optical polymer films, Appl. Phys. Lett. 66 (1995) 1166–1168, https://doi.org/10.1063/1.113845.
[8] P. Rochon, E. Batalla, A. Natansohn, Optically induced surface gratings on azoaromatic polymer films, Appl. Phys. Lett. 66 (1995) 136–138, https://doi.org/10.1063/1.113541.
[9] M.-H. Li, P. Keller, B. Li, X. Wang, M. Brunet, Light-driven side-on nematic elastomer actuators, Adv. Mater. 15 (2003) 569–572, https://doi.org/10.1002/adma.200304552.
[10] Y. Yu, M. Nakano, T. Ikeda, Directed bending of a polymer film by light, Nature. 425 (2003) 145–145. https://doi.org/10.1038/425145a.
[11] M. Camacho-Lopez, H. Finkelmann, P. Palffy-Muhoray, M. Shelley, Fast liquid-crystal elastomer swims into the dark, Nat. Mater. 3 (2004) 307–310, https://doi.org/10.1038/nmat1118.
[12] C.J. Barrett, A.L. Natansohn, P.L. Rochon, Mechanism of optically inscribed high-efficiency diffraction gratings in azo polymer films, J. Phys. Chem. 100 (1996) 8836–8842, https://doi.org/10.1021/jp953300p.
[13] C.J. Barrett, P.L. Rochon, A.L. Natansohn, Model of laser-driven mass transport in thin films of dye-functionalized polymers, J. Chem. Phys. 109 (1998) 1505–1516, https://doi.org/10.1063/1.476701.
[14] D. Han, X. Tong, Y. Zhao, T. Galstian, Y. Zhao, Cyclic azobenzene-containing side-chain liquid crystalline polymers: synthesis and topological effect on mesophase transition, order, and photoinduced birefringence, Macromolecules 43 (2010) 3664–3671, https://doi.org/10.1021/ma100246c.
[15] Y. Zakrevskyy, J. Stumpe, B. Smarsly, C.F.J. Faul, Photoinduction of optical anisotropy in an azobenzene-containing ionic self-assembly liquid-crystalline material, Phys.

Rev. E 75 (2007), https://doi.org/10.1103/PhysRevE.75.031703 031703.
[16] S. Xiao, X. Lu, Q. Lu, B. Su, Photosensitive liquid-crystalline supramolecules self-assembled from ionic liquid crystal and polyelectrolyte for laser-induced optical anisotropy, Macromolecules 41 (2008) 3884–3892, https://doi.org/10.1021/ma800059x.
[17] T. Ikeda, O. Tsutsumi, Optical switching and image storage by means of azobenzene liquid-crystal films, Science (80-.). 268 (1995) 1873–1875. https://doi.org/10.1126/science.268.5219.1873.
[18] L.M. Blinov, M.V. Kozlovsky, M. Ozaki, K. Skarp, K. Yoshino, Photoinduced dichroism and optical anisotropy in a liquid-crystalline azobenzene side chain polymer caused by anisotropic angular distribution of trans and cis isomers, J. Appl. Phys. 84 (1998) 3860–3866, https://doi.org/10.1063/1.368565.
[19] I. Zebger, M. Rutloh, U. Hoffmann, J. Stumpe, H.W. Siesler, S. Hvilsted, Photoorientation of a liquid-crystalline polyester with azobenzene side groups: effects of irradiation with linearly polarized red light after photochemical pretreatment †, Macromolecules 36 (2003) 9373–9382, https://doi.org/10.1021/ma034517h.
[20] P. Attri, E.H. Choi, Influence of reactive oxygen species on the enzyme stability and activity in the presence of ionic liquids, PLoS One 8 (2013) e75096, https://doi.org/10.1371/journal.pone.0075096.
[21] P. Attri, S.-H. Lee, S.W. Hwang, J.I.L. Kim, S.W. Lee, G.-C. Kwon, E.H. Choi, I.T. Kim, Elucidating interactions and conductivity of newly synthesised low bandgap polymer with protic and aprotic ionic liquids, PLoS One 8 (2013) e68970, https://doi.org/10.1371/journal.pone.0068970.
[22] P. Attri, K.Y. Baik, P. Venkatesu, I.T. Kim, E.H. Choi, Influence of hydroxyl group position and temperature on thermophysical properties of tetraalkylammonium hydroxide ionic liquids with alcohols, PLoS One 9 (2014) e86530, https://doi.org/10.1371/journal.pone.0086530.
[23] X. Pan, S. Xiao, C. Wang, P. Cai, X. Lu, Q. Lu, Photoinduced anisotropy in an azo-containing ionic liquid–crystalline polymer, Opt. Commun. 282 (2009) 763–768, https://doi.org/10.1016/j.optcom.2008.11.013.
[24] F. Zhao, Z. Pan, C. Wang, Y. Zhou, M. Qin, Third-order nonlinear optical properties of an azobenzene-containing ionic liquid crystalline polymer, Opt. Quantum Electron. 46 (2014) 1491–1498, https://doi.org/10.1007/s11082-013-9863-1.
[25] I.T. Kim, G.C. Kwon, E.H. Choi, S.H. Lee, Y.S. Kim, J.H. Kim, J.H. Cha, S.H. Kim, P. Attri, Interaction studies between newly synthesized photosensitive polymer and ionic liquids, Int. J. Polym. Sci. 2015 (2015) 1–8, https://doi.org/10.1155/2015/461974.
[26] D.U. Lee, J.Y. Jeong, J.W. Han, G.C. Kwon, P. Attri, I.T. Kim, Effect of ionic liquids on the physical properties of the newly synthesized conducting polymer, Int. J. Polym. Sci. 2018 (2018) 1–8, https://doi.org/10.1155/2018/8275985.
[27] S. Jeong, J.H. Yoon, P. Attri, I.T. Kim, Changes in the physical properties of low bandgap polymer after interaction with ionic liquids, J. Saudi Chem. Soc. 25 (2021), https://doi.org/10.1016/j.jscs.2021.101227 101227.
[28] S. Kim, P. Attri, I. Kim, Improvement in the diffraction efficiency of a polymer using an ionic liquid, J. Serbian Chem. Soc. 83 (2018) 213–220, https://doi.org/10.2298/JSC170527107K.
[29] I. Tochitsky, M.R. Banghart, A. Mourot, J.Z. Yao, B. Gaub, R. H. Kramer, D. Trauner, Optochemical control of genetically engineered neuronal nicotinic acetylcholine receptors, Nat. Chem. 4 (2012) 105–111, https://doi.org/10.1038/nchem.1234.